Numerical Simulation of Mixed Convective Flow Over a Three-Dimensional Horizontal Backward Facing Step

J. G. Barbosa Saldana
Graduate Research Assistant

N. K. Anand
Professor and Assistant Dean for Graduate Programs

Department of Mechanical Engineering,
Texas A&M University,
College Station, TX 77843, USA

V. Sarin
Assistant Professor
Department of Computer Science,
Texas A&M University,
College Station, TX 77843, USA

Laminar mixed convective flow over a three-dimensional horizontal backward-facing step heated from below at a constant temperature was numerically simulated using a finite volume technique and the most relevant hydrodynamic and thermal features for air flowing through the channel are presented in this work. The channel considered in this work has an aspect ratio AR=4*, and an expansion ratio* ER=2*, while the total length in the streamwise direction is 52 times the step height* (L=52 s) *and the step length is equal to 2 times the step height* (l=2 s)*. The flow at the duct entrance was considered to be hydrodynamically fully developed and isothermal. The bottom wall of the channel was subjected to a constant high temperature while the other walls were treated to be adiabatic. The step was considered to be a thermally conducting block.*
[DOI: 10.1115/1.2005272]

Keywords: Numerical Simulation, Backward-Facing Step, Mixed Convection

Introduction

Separation and reattachment flows is a phenomenon that is found in several industrial devices such as in pieces of electronic cooling equipment, cooling of nuclear reactors, cooling of turbines blades, flow in combustion chambers, flow in wide angle diffusers, and valves. In other situations the separation is induced in order to induce more favorable heat transfer conditions as in the case of compact heat exchangers [1–3].

In the last decade several numerical studies have been conducted to gain a better knowledge and understanding of the hydrodynamic and thermal aspect of the separated flow. In this aspect the backward-facing step has been the main target of several researchers. Even though the geometry is simple it is rich in physics as it captures complex flow and heat transfer features associated with separation and reattachment. For this reason flow over a backward facing step has been used as a benchmark problem for validating numerical codes and numerical procedures [4].

The recent developments in terms of computing speed and memory storage has permitted the solution to problems that demands an extremely high computational resources as in the case of numerical simulations of three-dimensional flows, including fluid flow and heat transfer phenomenon over a three-dimensional backward facing step problem [5–7]. However, none of the previous cited publications include the effects of buoyant forces or mixed convective flow, even though the effects of buoyancy forces become significant when dealing with laminar flow regime with strong temperature gradients.

The mixed convective flow over a three-dimensional backward facing step is not a very common topic found in the literature. Nie, Armaly, Li, and co-workers [8,9] have considered the effect of buoyancy force (mixed convection effects) in vertical ducts wherein the gravitational vector and flow direction are parallel.

Iwai et al. studied mixed convection in vertical ducts with backward facing step by varying the duct angle of inclination [2]. However, their study was confined to extremely weak buoyancy forces. For example, when the backward facing step is aligned with the horizontal axis the modified Richardson number was chosen to be equal to 0.03 (Ri^*=0.03). This value is associated with not strong enough buoyancy effects to alter the velocity field and temperature distributions from the pure forced convection values. Therefore, the flow in the cited report can be judged and qualified as being a pure forced convective flow.

Thus the work that comes close to the configuration considered in this study is that of Iwai et al. [2]. Hence it is concluded that there is no work reported on mixed convective flows over a horizontal three-dimensional backward facing step to date in the literature.

In this work, numerical simulation of three-dimensional mixed convective air flow over a horizontal backward facing step heated from below at a constant temperature is presented. The simulation is carried out for dominant free convective flow and the results for limiting cases are compared with those of pure force convective three-dimensional flow. Also, the back step is considered as a conductive block which is another unique aspect of this study.

Model Description and Numerical Procedure

The geometry considered in this study is shown in Fig. 1. The duct aspect ratio and expansion ratio were fixed in relation to the step height (s) as AR=4 and ER=2, respectively. The total length of the channel is equal to 52 times the step height L=52 s and the length of the step is fixed as 2 times the step height l=2 s. This particular geometry was chosen to study the strong three-dimensional behavior of the flow over the backward facing step.

Flow was assumed to be steady and the Boussinesq approximation was invoked. Based on these simplifying assumptions the steady three-dimensional mass conservation, momentum equations, and energy equation governing the fluid flow and heat transfer problem are reduced to the following forms [10,11]:
continuity equation:

$$\frac{\partial(\rho u)}{\partial x}+\frac{\partial(\rho v)}{\partial y}+\frac{\partial(\rho w)}{\partial z}=0, \tag{1}$$

X momentum equation:

Contributed by the Heat Transfer Division for publication in the JOURNAL OF HEAT TRANSFER. Manuscript received: May 27, 2004. Final manuscript received: April 27, 2005. Review conducted by: Sumanta Acharya.

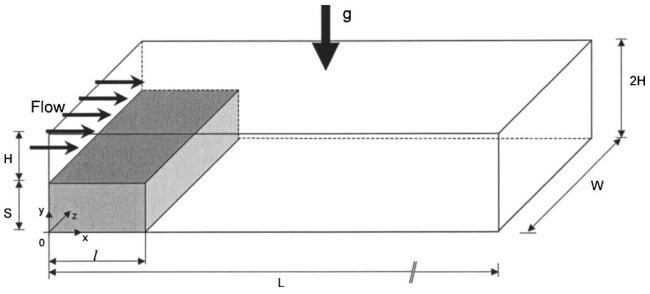

Fig. 1 Schematic of the three-dimensional backward facing step

$$\left(u\frac{\partial(\rho u)}{\partial x}+v\frac{\partial(\rho u)}{\partial y}+w\frac{\partial(\rho u)}{\partial z}\right)=-\frac{\partial p}{\partial x}+\left[\frac{\partial}{\partial x}\left(\mu\frac{\partial u}{\partial x}\right)+\frac{\partial}{\partial y}\left(\mu\frac{\partial u}{\partial y}\right)+\frac{\partial}{\partial z}\left(\mu\frac{\partial u}{\partial z}\right)\right], \tag{2}$$

Y momentum equation:

$$\left(u\frac{\partial(\rho v)}{\partial x}+v\frac{\partial(\rho v)}{\partial y}+w\frac{\partial(\rho v)}{\partial z}\right)=-\frac{\partial p}{\partial y}+\rho_0\beta(T-T_0)g_y+\left[\frac{\partial}{\partial x}\left(\mu\frac{\partial v}{\partial x}\right)+\frac{\partial}{\partial y}\left(\mu\frac{\partial v}{\partial y}\right)+\frac{\partial}{\partial z}\left(\mu\frac{\partial v}{\partial z}\right)\right], \tag{3}$$

Z momentum equation:

$$\left(u\frac{\partial(\rho w)}{\partial x}+v\frac{\partial(\rho w)}{\partial y}+w\frac{\partial(\rho w)}{\partial z}\right)=-\frac{\partial p}{\partial x}+\left[\frac{\partial}{\partial x}\left(\mu\frac{\partial w}{\partial x}\right)+\frac{\partial}{\partial y}\left(\mu\frac{\partial w}{\partial y}\right)+\frac{\partial}{\partial z}\left(\mu\frac{\partial w}{\partial z}\right)\right], \tag{4}$$

energy equation:

$$\left(u\frac{\partial(\rho CpT)}{\partial x}+v\frac{\partial(\rho CpT)}{\partial y}+w\frac{\partial(\rho CpT)}{\partial z}\right)=\left[\frac{\partial}{\partial x}\left(k\frac{\partial T}{\partial x}\right)+\frac{\partial}{\partial y}\left(k\frac{\partial T}{\partial y}\right)+\frac{\partial}{\partial z}\left(k\frac{\partial T}{\partial z}\right)\right]. \tag{5}$$

The Y momentum Eq. (2) contains the buoyancy effects and according to the Boussinesq approximation the density variation due to the buoyancy effect is related to the volumetric thermal expansion coefficient (β) of the fluid.

At the channel entrance the flow was treated as a three-dimensional fully developed flow [12] with uniform temperature. No-slip condition was applied at the channel walls, including the step. The bottom wall of the channel ($0\leq x\leq L$; $0\leq z\leq W$) was subjected to a constant temperature (T_w) and the rest of the walls were treated as adiabatic.

In this work the step was considered to be conducting with a thermal conductivity k_s. The conjugate problem of conduction convection at the solid–fluid interface of the step was solved by a pseudo-solid-specific heat method as suggested by Xi and Han [13].

The physical properties of air in the numerical procedure were treated as constants and evaluated at the inlet temperature $T_0=293$ K, as $\rho=1.205$ kg/m^3, $\mu=1.81\times10^{-5}$ kg/m s, $C_p=1005$ J/kg K, $k_f=0.0259$ W/m K, and $\beta=0.003\,41$ K^{-1}. The thermal conductivity of the back step was set equal to $k_s=386$ W/m K.

The flow rate in the duct entrance was fixed such that the Reynolds number (Re) would have a constant value of 200 for all the numerical simulations. The Reynolds number was computed based on the inlet bulk velocity U_o and the channel height. The effects of the buoyancy forces on the velocity field and the temperature distribution was studied by varying the Richardson number from Ri=0 to 3 and then selecting the appropriate value for the bottom wall temperature (T_w).

A finite volume technique was implemented for discretizing the momentum and energy equations inside the computational domain. The SIMPLE algorithm was used to link the pressure and velocity fields. Solution to the one-dimensional convection-diffusion equation at the control volume interfaces was represented by the power law [14]. Velocity nodes were located at staggered locations in each coordinate direction while pressure and temperature nodes as well as other scalar properties were placed at the main grid nodes. At the channel exit the natural boundary conditions

$$\left(\frac{\partial()}{\partial x}=0\right)$$

were imposed for all the variables [14]. In addition, the overall mass flow in and out of the domain were computed and its ratio was used to correct the outlet plane velocity at the channel exit as proposed by Versteeg and Malalasekera [15].

A combination of line-by-line solver and Thomas algorithm was implemented for each plane in x, y, and z coordinate directions for the computation of the velocity components, pressure, and temperature inside the computational domain. To ensure convergence when solving the mixed convective flow over a three dimensional horizontal backward facing step a severe underrelaxation for the velocity components ($\alpha_u=\alpha_v=\alpha_w=0.4$), pressure ($\alpha_p=0.4$) and temperature ($\alpha_T=0.4$) was imposed. Convergence was declared when residuals for the velocity components (R_u,R_v,R_w) and for the pressure (R_p) were less than 1×10^{-8} and 1×10^{-10}, respectively. For the temperature field the convergence criterion required that the maximum relative change in temperature between successive iterations is less than 1×10^{-6}. The definitions for the residuals adopted for the velocity components, pressure, and temperature are presented in Eqs. (6), (7), and (8), respectively, [16]:

$$R_\phi=\frac{\sum_{\text{nodes}}|a_p\phi_p|-\left[\sum|a_{nb}\phi_{nb}|-A(p_\phi-p_{\phi+1})-b\right]_{\text{nodes}}}{\sum_{\text{nodes}}|a_p\phi_p|}\leq\varepsilon_\phi, \tag{6}$$

$$R_p=\sum_{\text{nodes}}|\rho A[(u_w-u_e)+(v_s-v_n)+(w_b-w_t)]|\leq\varepsilon_p, \tag{7}$$

$$R_T=\left(\left|\frac{T^{n+1}_{k,j,i}-T^{n}_{k,j,i}}{T^{n+1}_{k,j,i}}\right|\right)\leq\varepsilon_T. \tag{8}$$

In the Eq. (6) ϕ represents the u, v, and w velocity components and a coefficients are defined in context of the finite volume discretization technique [14].

A nonuniform grid was considered for solving the problem. In this sense, at the channel walls and at the edge of the step the grid was composed by small-size control volumes (fine grid) and the control volume size increased far away from the solid walls. The grid size was deployed by means of a geometrical expansion factor, such that each control volume is a certain percentage larger than its predecessor.

The grid independence study was conducted by using several grid densities for the most severe parametric values (Ri=3 and Re=200) considered in this study. The average Nusselt number

Table 1 Grid independence study

Grid Size (x-y-z):(100-40-40) Expansion factor (x-y):(1.025-1.35)				
Expansion factor for Z	Nusselt average at exit	% diff	u-max at the exit	% diff
Uniform grid	4.7743		0.1248	
1.04	4.5016	6.05	0.1326	5.91
1.08	4.1798	7.69	0.1324	0.11
1.10	4.0263	3.81	0.1326	0.08
1.12	3.8812	3.73	0.1326	0.0
1.14	3.7462	3.60	0.1324	0.15
1.16	3.6223	3.42	0.1323	0.07
1.18	3.5098	3.20	0.1322	0.07
1.20	3.4085	2.97	0.1322	0.0

distribution (Nu) and the maximum velocity (u_{max}) at the channel exit were monitored to declare grid independence.

A grid size of $100\times40\times40$ was chosen as the base case. By keeping the number of grid points constant several runs were made by varying the expansion factor in the z direction. The variation of the expansion factor did not increase the number of nodes but affected their allocation in the computational domain. In this sense, as the expansion factor increases a fine grid distribution is realized in the vicinity of the solid walls, so velocity, pressure, and temperature gradients in these specific zones could be resolved with greater accuracy.

Once the appropriate value for the expansion factor was obtained such that the monitored parameters have small deviations, the next step was to add grid points in each direction. However, further addition of grid points to the grid in the x, y, and z directions resulted in less than 1% change in the averaged Nusselt number and maximum u velocity at the channel exit. Accordingly, a nonuniform grid of $100\times40\times40$ and expansion factors $e_x=1.025$, $e_y=1.35$, and $e_z=1.20$ was chosen to make parametric runs. The result of this grid independence study is summarized in Table 1.

Lack of previous experimental or numerical data in the literature for the problem in question precludes the direct numerical validation of the numerical code developed for solving the mixed convective flow over a three dimensional horizontal backward facing step. Hence, two closely related problems to the mixed convective flow over a three dimensional backward facing step were considered to validate the numerical code developed for this research. For each verification test the hydrodynamic and thermal flow features were compared with the previously published works in the literature.

Test Case #1. The first test case was that for simulating pure forced convective flow over a three-dimensional backward facing step subjected to constant heat flux heating along the bottom wall [6]. The numerical predictions of reattachment lengths and Nusselt number distributions using the developed code was compared with the experimental data for Re=343 and numerical predictions for Re=400 presented by Nie and Armaly [6]. The comparisons are shown in Figs. 2 and 3.

Due to the symmetry for pure forced convection the literature presents values for half of the channel in the spanwise direction. However, this assumption was not considered in this research and computations were made by considering the entire spanwise width of the channel. In order to be consistent with the format in the referenced cited, the results are presented for only half of the channel width in Figs. 2 and 3.

The numerical predictions using the code developed for this research very closely agrees with both the experimental and numerical results in the published literature shown in Figs. 2 and 3.

Test Case # 2. The second test case was that for simulating mixed convective flow in straight horizontal channel with no

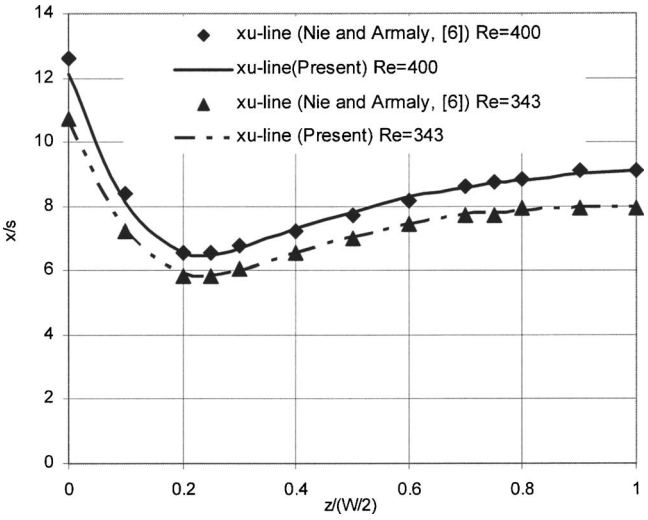

Fig. 2 x_u line for the stepped wall ($z/W=0$ wall and $z/W=1$ central plane)

blockage heated from below by subjecting the wall to a constant temperature [17]. The width to height channel's ratio was equal to 2. The numerical predictions using the code developed for this research closely agreed with the numerical predictions in the literature as shown in Fig. 4.

Results and Discussion

According to earlier studies [1,3–7], it is known that the flow over the backward facing step channel is extremely sensitive to the abrupt geometrical changes at the step. Downstream of the step and just behind the primary recirculation zone, the velocity profile is reattached and redeveloped approaching that of a fully developed flow as fluid flows towards the channel exit. However, the behavior described earlier for a pure force convective flow is completely distorted in presence of buoyancy forces. The last scenario considered is a mixed convective problem and is the central theme for this work.

The mixed convective flow is a process in which both the forced and the buoyancy effects are of significant importance in the convective process and primarily occurs in laminar and tran-

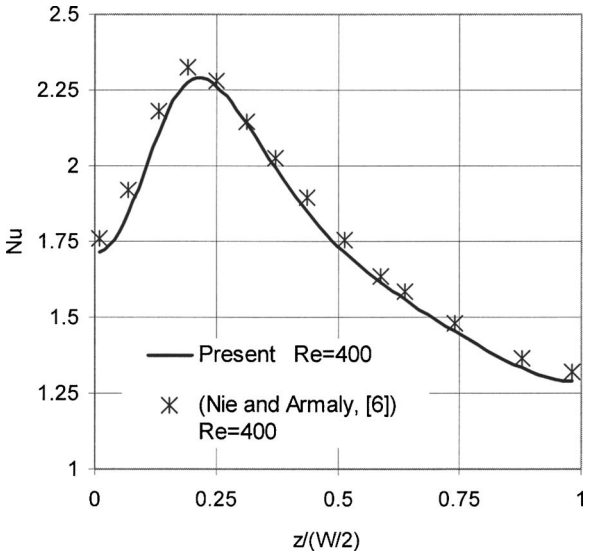

Fig. 3 Local Nusselt number distribution for the stepped wall at $x/s=6.6$ ($z/W=0$ wall and $z/W=1$ central plane)

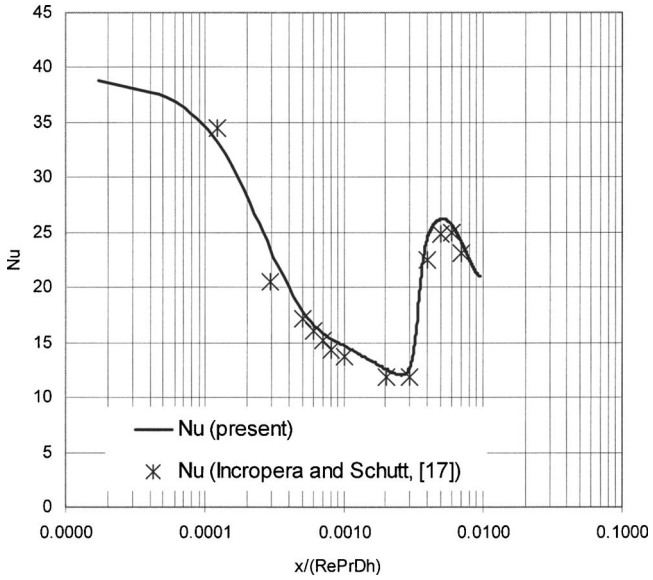

Fig. 4 Average Nusselt number for a mixed convective flow through a straight rectangular channel $Gr=1.55\times10^6$, Re=500 and Pr=6.5

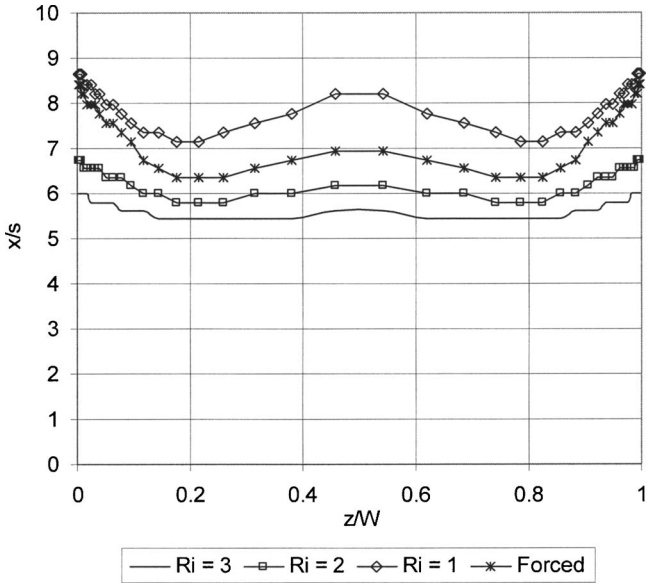

Fig. 5 x_u-line distribution for mixed convection over a 3D backward facing step

sitional flow regimes. Therefore, for all numerical simulations considered in this study the Reynolds number (Re) was fixed to be Re=200.

The variation in buoyancy forces was accomplished by altering the imposed temperature along the bottom wall which in turn alters the Richardson number (Ri). Mixed convective effects on the flow were studied by simulating flows for three different Richardson numbers (Ri=1, 2, and 3). When Ri=1 the forced and free convective forces are comparable and, as Ri increases the free convective effects become dominant over forced convective effects in the flow. The extreme case in this study is for Ri=3, where the free convective effects strongly prevail over the forced convective effects.

The mixed convective effects were studied by monitoring the so-called x_u line, the average Nusselt number, and some velocity profiles at specific planes by comparing with the results for mixed convective flow and those for pure forced convective flow.

In a two-dimensional problem flow over a backward facing step, the point where the shear stress is equal to zero is used to locate the reattachment length and to allocate the primary recirculation zone downstream of the step. However, for a three-dimensional flow the same definition represent a point in a horizontal plane and cannot be used to demarcate the recirculation zone. The common assumption for delimiting the recirculation zone in a three-dimensional case is the distribution in the spanwise direction of points along the axial direction where the streamwise component of the shear stress at the wall is equal to zero. Therefore, the limiting primary recirculation zone is bounded by a line in the spanwise direction named the x_u line.

Figure 5 shows the x_u line for different mixed convective and pure forced convective flows. The x_u lines present a symmetric behavior with respect to the middle plane in the spanwise direction. A minimum value is located approximately at $z/W=0.2$ and $z/W=0.8$. This effect is associated with the influence of the viscous effects and the no slip condition imposed at the lateral walls. The larger reattachment point is along the lateral walls.

For Ri=1 a very similar behavior as the pure forced convective flow is found. However, the location of x_u line for mixed convective flow Ri=1 is pushed further downstream. The mixed convection in ducts presents two different structures or convective rolls, and depending on the effects of the mixed convection the rolls can be transverse or longitudinal in nature [18]. The onset of transverse rolls occurs at low Grashof numbers (Gr). Therefore for Ri=1, the presence of longitudinal rolls is the reason why the x_u line is displaced downstream of the channel inlet ($x/s=0$).

On the other hand, for Ri=2 and 3 the location of x_u line is upstream of the x_u-line location for Ri=0. It is evident from the Fig. 5, that when Ri increases the recirculation zone is shortened due to the presence of strong buoyancy forces and higher v velocity components in the vicinity of the heated wall.

The average along the span-wise direction of the streamwise shear stress component at the channel's bottom wall is presented in Fig. 6. The negative values in Fig. 6 are associated with the primary recirculation zone and the point where τ_{wx} changes to a positive value could be interpreted as "*the averaged reattachment point*." This point is shifted upstream if Ri is large (Ri=3) and the

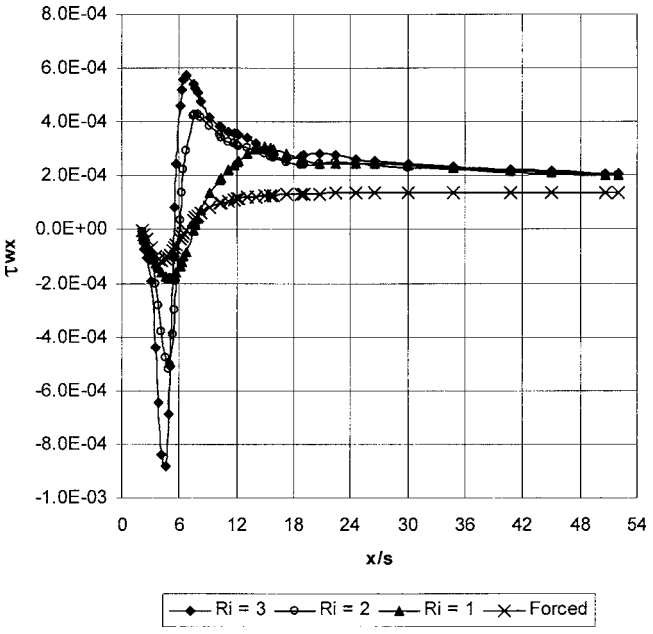

Fig. 6 Spanwise average of the streamwise shear stress component along the bottom wall

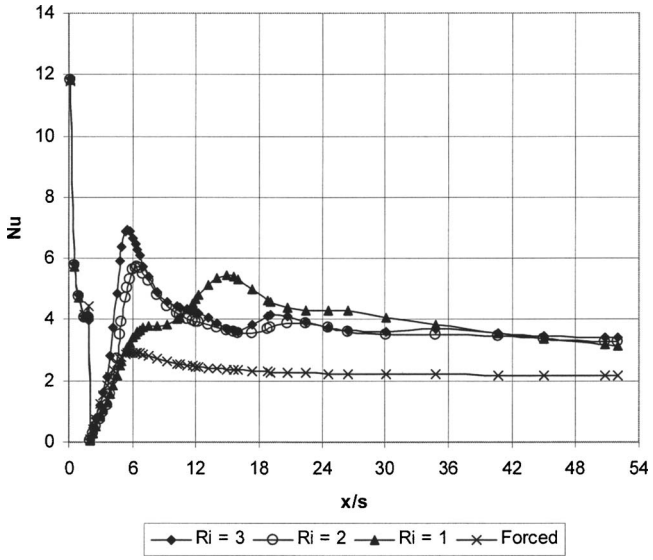

Fig. 7 Spanwise averaged Nusselt number distribution for the mixed convective flow over a 3D backward facing step

farthest point downstream happens to be for Ri=1 as a consequence of the earlier discussion following Fig. 5.

The spanwise averaged Nusselt number distribution for the mixed convective flow in a channel with a backward step is presented in Fig. 7. The averaged Nusselt number distribution at the entrance of the backward facing step channel has a high value and then monotonically decreases. At the edge of the step a dramatic change in the averaged Nusselt number distribution was found due to the flow separation and the abrupt change in the channel geometry. Figure 7 shows a similar tendency for the averaged Nusselt number distributions for the three mixed convective cases in consideration and the higher values are associated to higher Ri numbers.

For Ri=1, the location of the maximum Nusselt number is found further downstream of the step (step ends at $x/s=2$) while for Ri=3 and 2 the location of the maximum was found in the proximity of the step. Hence, the location of the maximum spanwise averaged Nusselt number shifts upstream with increase in Ri. After reaching a maximum value the Nusselt number decreases toward its fully developed value at the channel exit. It is also observed in this figure that after reaching the minimum value just behind the step, the Nusselt number distribution sharply increases to reach its maximum value inside the primary recirculation zone for Ri=3 and Ri=2. For Ri=1 the change from the minimum value of Nusselt number to the maximum is not as sharp as for Ri=3 and 2 due to presence of longitudinal rolls as described earlier (Fig. 5).

According to Fig. 7 the spanwise averaged Nusselt number distribution for pure forced convective flow has a similar behavior as for the mixed convective flow, but the spanwise values for the averaged Nusselt number distribution are considerably smaller for the pure forced convection than those for the mixed convection case. The minimum value in the spanwise averaged Nusselt number distribution for forced convection happens just behind the step

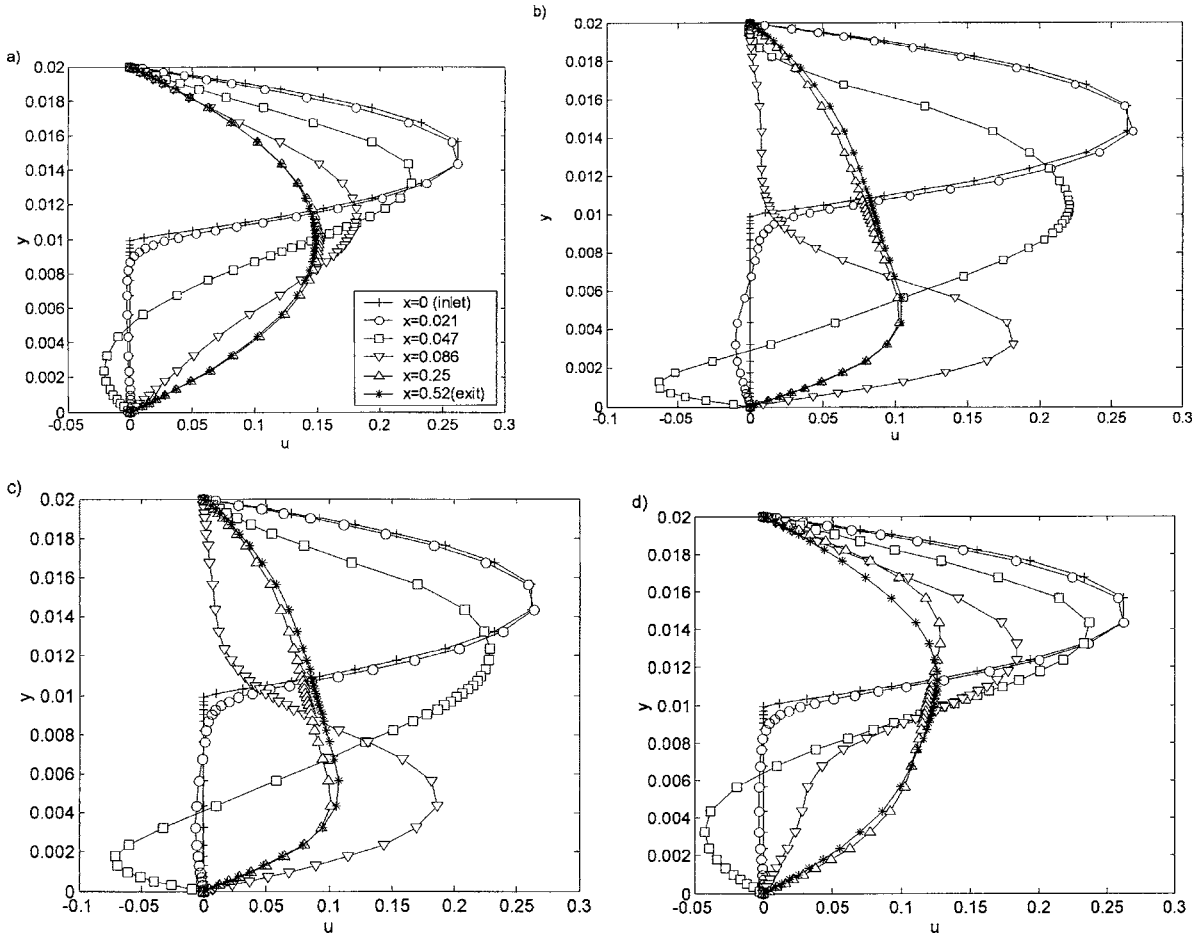

Fig. 8 *u*- velocity profiles at plane *z*=0.02 at different *x* positions (a) forced convection (b) Ri=3, (c) Ri=2, (d) Ri =1

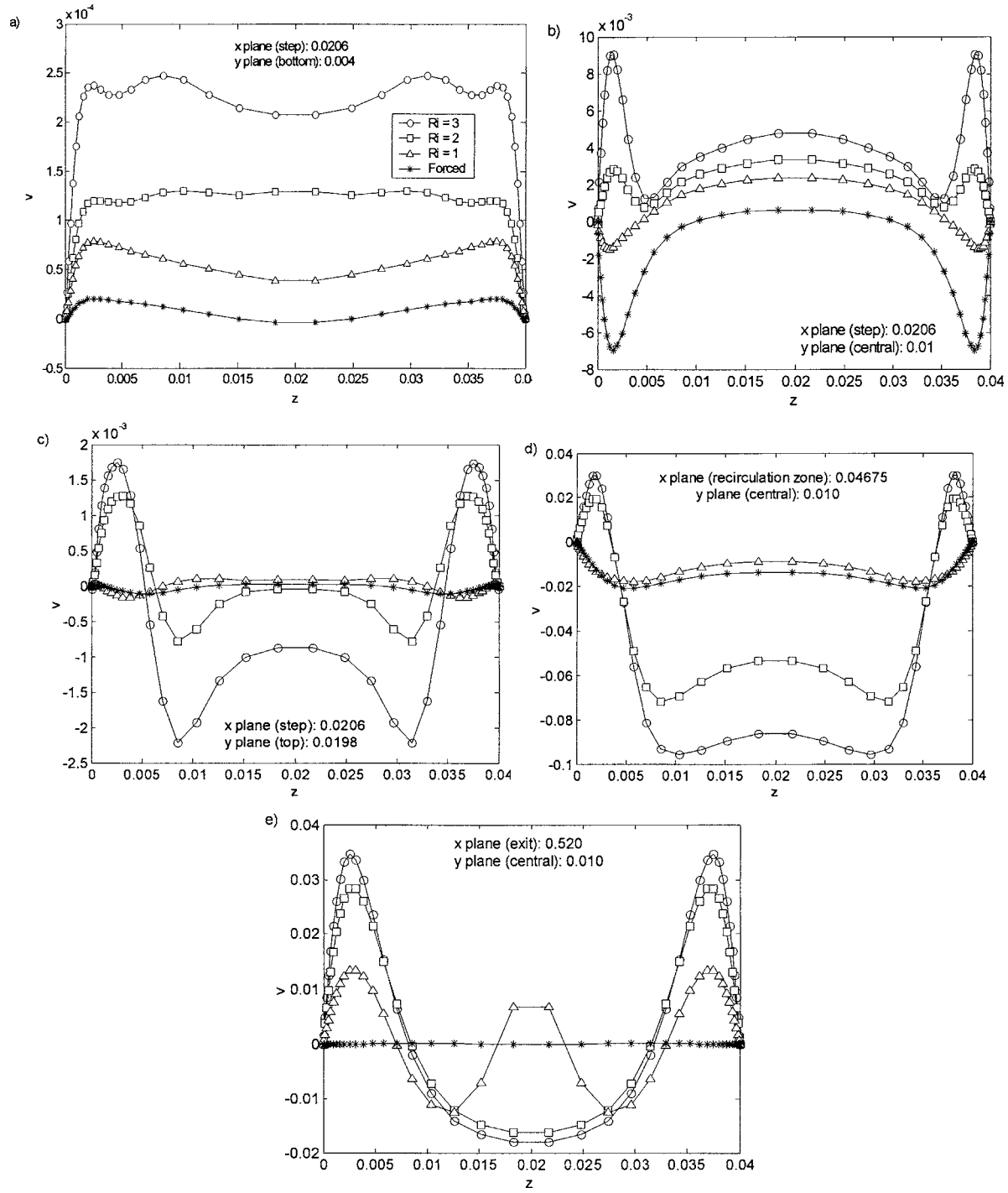

Fig. 9 *v* velocity at different *x* and *y* planes

and its maximum is reached inside the primary recirculation zone, and decreases monotonically towards its fully developed value at the channel exit.

Velocity distributions for each of the velocity components are presented in Figs. 8–10 in order to study the influence of the buoyancy forces on the flow field. Figure 8 shows the u velocity component for the central plane in the spanwise direction ($z/W=0.5$) at different x planes for pure forced convective flow and mixed convective flow. As previously mentioned, at the inlet ($x=0$) the flow is considered as hydrodynamically fully developed for all cases considered in this study.

In the vicinity of the step at $x=0.02$, the u velocity component has a slight deviation from the hydrodynamically fully developed flow values and the velocities at this point are slightly less than that for $x=0$ in region above the step. Also, u values were negative near the bottom of the channel and this effect is most pronounced for the case of Ri=3.

At a constant value of $x=0.047$ the recirculation of the flow becomes evident along the bottom of the channel. Also, the negative value of u next to the bottom wall of the channel increases with increase in Ri. On the other hand the maximum value of the u component in the positive direction occurs for the pure forced convective flow. As Ri increases, the vertical size of the recirculation zone is reduced. This effect is related to the buoyancy forces in the flow.

Figure 8(b) reveals the presence of a small recirculation zone

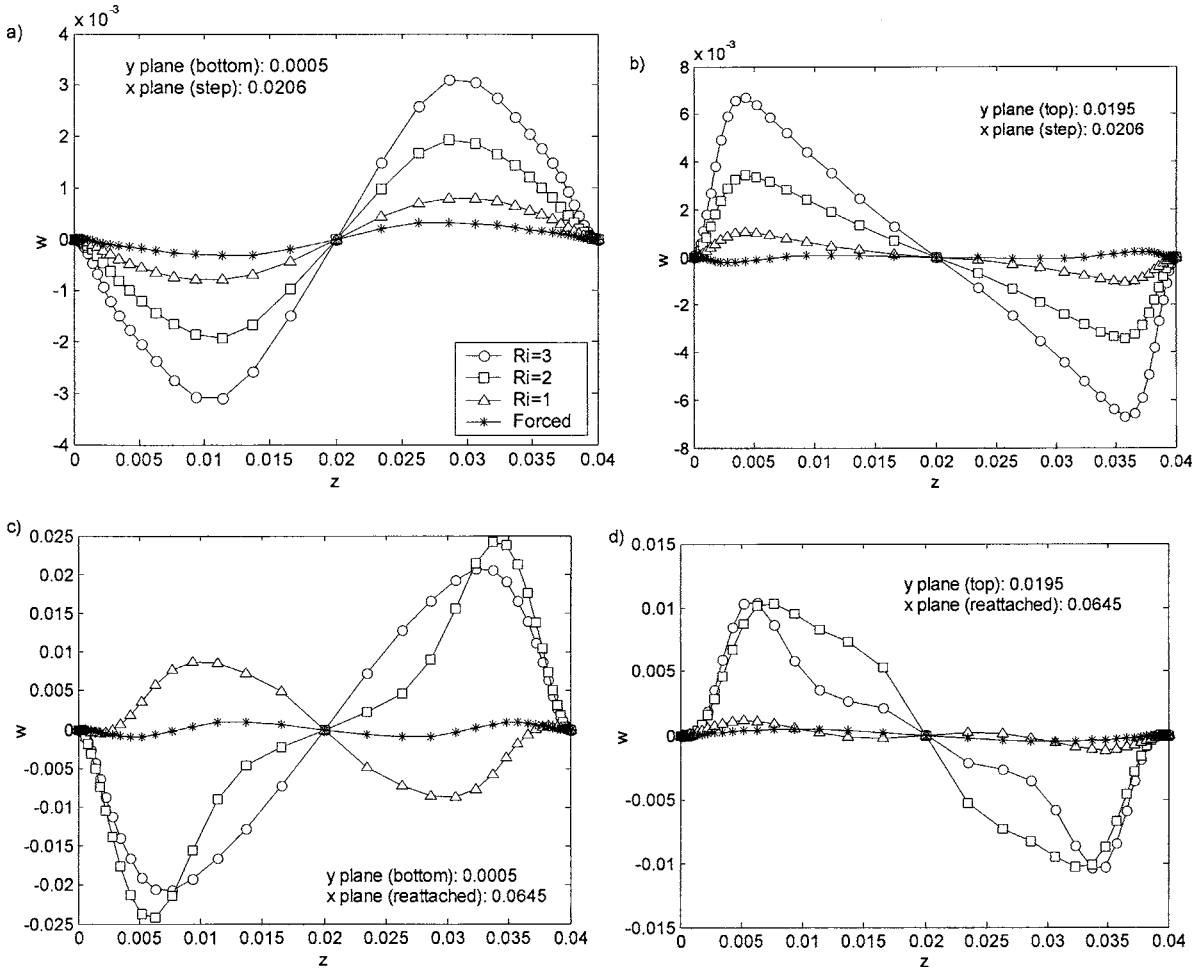

Fig. 10 ***w*** **velocity component at different** ***x*** **and** ***y*** **planes**

attached to the roof of the channel at $x=0.047$ and the effect extends up to $x=0.086$. This effect was found only for the Ri=3 and is due to the strength of the mixed convective flow in this case.

The u velocity profile at $x=0.25$ (half of the channel in the streamwise direction) reveals that for pure forced convective flow the u velocity component begins to show a fully developed behavior. For Ri=1 the u-velocity components tends to approach fully developed velocity profile. For Ri=3 and Ri=2 the velocity profile behavior is very different to be a fully developed flow. The maximum in the velocity profile is shifted towards the bottom of the channel. This behavior will be explained below.

It is evident from Fig. 8 that the length of the channel is long enough to accommodate fully developed flow for pure forced convection (Ri=0). None of the mixed convective flow cases considered in this study was able to reach the hydrodynamically fully developed conditions at the channel exit. The case of Ri=1 was the one of the mixed convective cases that appeared to be approaching fully developed flow conditions at the channel exit. The u-velocity components at the channel exit for mixed convective cases were found to be nonsymmetric with respect to the y axis. Even though the fully developed conditions were not achieved, it becomes clear that at the channel exit the u-velocity component does not present any negative values. Hence, at the channel exit a possible inflow condition is discarded and then the outflow boundary conditions imposed to the numerical code does not have a negative impact on the numerical predictions.

Figure 9 presents the v-velocity distribution. In these figures, the plane $y=0.01$ is the central plane while $y=0.004$ is a plane near to the bottom wall and $y=0.0198$ is a plane near to the top wall.

The magnitude of the velocity v component is extremely small near the top and bottom walls. It should be noted that higher values for the v component are for Ri=3 where the buoyancy effects dominate.

Figure 9(a) shows that for Ri=3 the v-velocity component values are three times larger than the values for pure forced convective flow. This effect is associated with the strength of the mixed convective flow as it was mentioned before; the effect of mixed convection is to reduce the size of the recirculation zone in both streamwise and vertical directions.

Figure 9(b) shows that at the edge of the back step, the line for pure forced convection does not have positive values for the v-velocity component, but the lines for Ri=3 and Ri=2 have the opposite behavior. In others words, at the edge of the step for pure forced convection the flow is descending while for mixed convection the flow is ascending due to the buoyancy forces. Figure 9(c) shows that at the top of the channel the v velocity has negative values along the spanwise direction and except a small region near the side walls where the values are positive.

Figure 9(d) shows the v velocity at x constant plane inside the primary recirculation zone and at the central constant y plane in the vertical direction. For Ri=3 and 2 the earlier mentioned effect of ascending flow near the side walls is observed. However, at the channel central region in the z-direction the v-velocity distribution shows high negative values and the flow is directed towards the

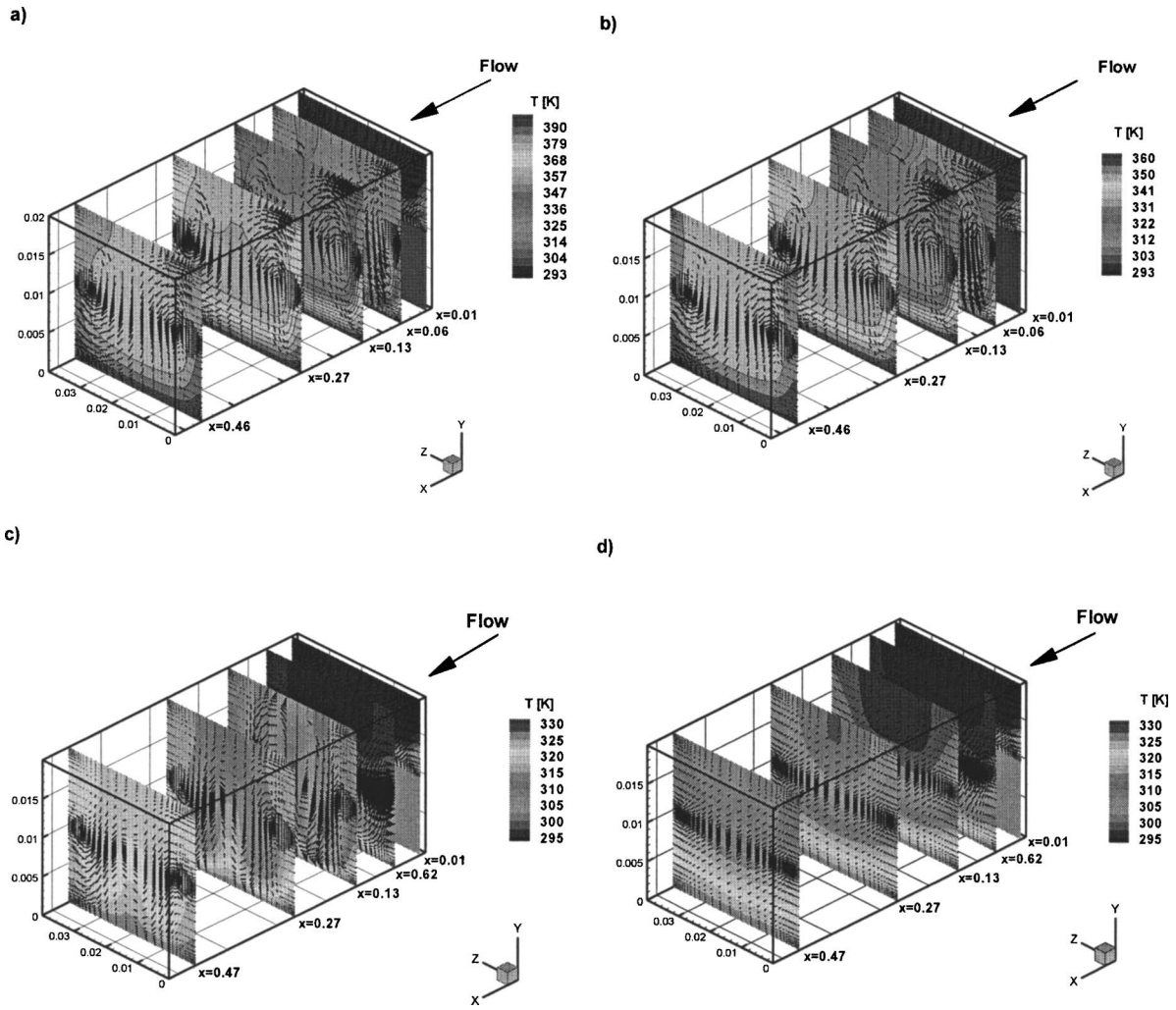

Fig. 11 Temperature contours and velocity vectors at constant *x* planes (a) Ri=3, (b) Ri=2, (c) Ri=1, (d) forced convection

bottom wall. This is the reason why the recirculation zone is not only reduced in the streamwise direction but also in the transverse direction (y direction).

Figure 9(e) confirms that at the channel exit the flow is fully developed for pure forced convective flow ($v=0$) and that for mixed convective flow, the v component of the velocity has considerable nonzero values. This figure also shows that for strong mixed convective flow (Ri=3 and Ri=2) positive values for the v-velocity component are present near the side walls and negative values are present in the middle of the channel. This is the reason why the maximum of u-velocity component in the central plane is shifted towards the bottom wall as seen in Figs. 8(b) and 8(c).

Figure 10 presents the spanwise velocity w distribution at different x and y planes. It is evident in Fig. 10 that for pure forced convective flow the change in the w-velocity component is minimal and also that the variation in w component in the spanwise direction is greater near the walls than in the middle of the channel. This behavior is associated with the formation of convective rolls in the flow. Even though the variation in the w-velocity component is minimal, this component cannot be neglected in the numerical discretization in order to save computational effort.

As expected, the higher values for the w-component velocities are associated with larger Ri values. In the vicinity of the back step [Figs. 10(a) and 10(b)] the w component of the velocity has extremely small values. Higher values for the w-velocity component occurs downstream of the backstep [Figs. 10(c) and 10(d)].

Analyzing Fig. 10 and considering the coordinate system proposed in Fig. 1 it is evident that near the top of the channel the w-velocity component acts towards the central plane in the spanwise direction ($z=0.02$), while near the bottom wall the flow is directed towards the side walls.

Figure 11 presents the temperature contours and the velocity vectors at different streamwise positions for the convective flows considered in this study.

A pair of longitudinal convective rolls is perfectly defined for Ri=3 and Ri=2 in Figs. 11(a) and 11(b). It is evident that the flow is ascending along the side walls and is moving towards the bottom wall near the middle plane in the spanwise direction ($z=0.02$). That is the reason why in Figs. 8(b) and 8(c) the maximum for the u velocity at the channel exit is shifted towards the bottom wall. For Ri=1 the longitudinal vortex are not completely defined even though the velocity structures tends to align with longitudinal vortices. For the pure forced convective case in Fig. 11(d) the flow structures do not show formation of the convective rolls, but they are more like a fully developed flow.

The temperature contours show the presence of high temperatures along the channel roof. According to the linear relationship between density and temperature this is an expected behavior. Flow with lower density and high temperature must be along the top wall of the channel. For the pure forced convective case the temperature contours reveals that the region of higher temperature are near to the heating zone.

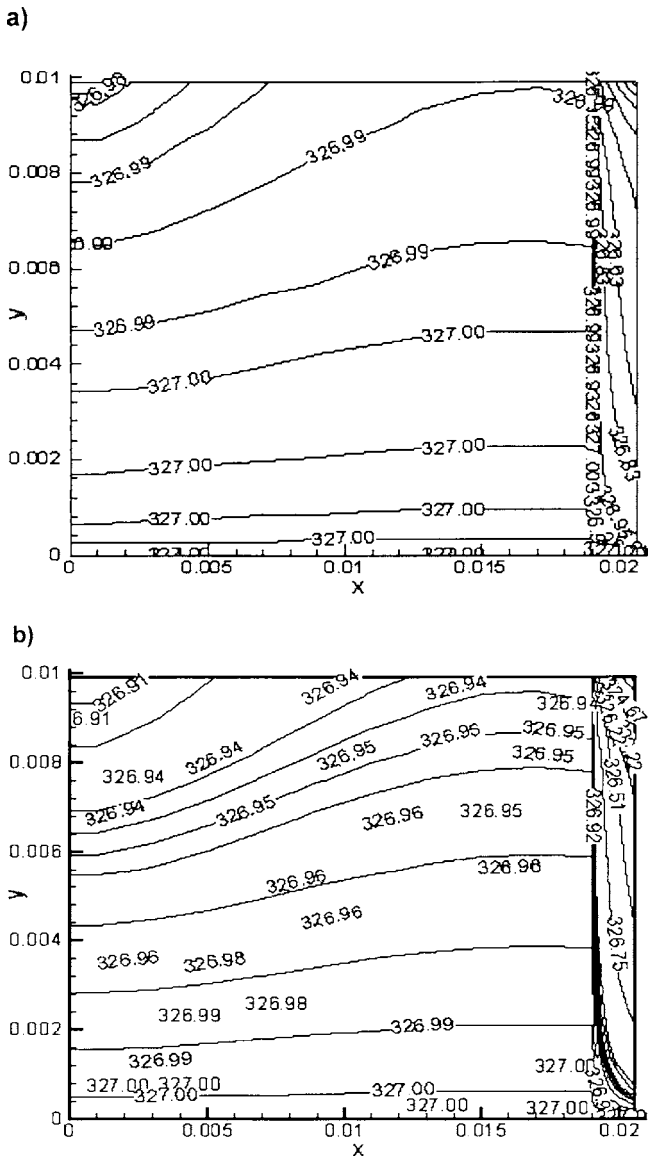

Fig. 12 Temperature distribution inside the back-step for the central plane z=0.02 (a) k_s=386 (copper) (b) k_s=64 (carbon steel AISI 1010)

The influence of the conducting block on the mixed convective flow was studied for two different block's thermal conductivity. Figure 12(*a*) shows the temperature distribution inside the block along the central plane in the spanwise direction for k_s =386 W/m K (copper). Similarly Fig. 12(*b*) for k_s=64 W/m K (carbon steel AISI 1010).

The thermal conductivity in the block does not impact the temperature distribution for mixed convective flow and the only effect is on the temperature distribution inside the back step. Even though the temperature gradients inside the block can be neglected it was found that a higher temperature gradient is found for the lower thermal conductivity (k_s=64 W/m K). It is important to mention here that the geometrical dimensions for the back step in the streamwise direction (x direction) is two times the step height while the total length of the channel is 52 times the step height.

Conclusions

The mixed convective flow over a three dimensional horizontal backward facing step heated from below was numerically simulated using a finite volume technique. The bottom wall of the channel was subjected to constant temperature. Numerical simulations were conducted for four different buoyancy parameters (Ri=Gr/Re^2) ranging from pure forced convective flow to mixed convective flow (Ri=0,1, 2, and 3).

The numerical results show that the velocity field and temperature distribution features for the mixed convective flow are significantly different from that for pure forced convective flow, even for small Ri. Hence, the effects of buoyancy forces should be considered in simulation of mixed convective flows.

The effect of increase in Richardson number (Ri) on the mixed convective flow not only decreased the size of the primary recirculation zone in both streamwise and transverse directions, but also moved the location of maximum in the averaged Nusselt number distribution and maximum in the averaged streamwise shear stress distribution further upstream.

At the channel exit the fully developed conditions are not achieved for mixed convective flows. It should be noted that for pure forced convective flow (Ri=0) the flow does achieve fully developed flow condition at the channel exit.

Acknowledgment

Support for this work by ANUIES/IPN Mexico is greatly appreciated.

Nomenclature

a = discretization coefficients
A = area
AR = aspect ratio, AR=W/s
b = linearization for the source term
C_p = specific heat
e = expansion factor
ER = expansion ratio, $ER=2H/(2H\text{-}s)$
g = acceleration due to gravity
Gr = Grashof number, $\mathrm{Gr}=g\beta\Delta Ts^3/\nu^2$
H = channel height at the inlet
k = thermal conductivity
L = total length of the channel, L=52 s
l = total length of the step, l=2 s
n = iteration number
Nu = average Nusselt number, $\mathrm{Nu}=(d\bar{T}/dy)|_{y=0}2H/(T_{\mathrm{wall}}-T_b)$
p = pressure
Pr = Prandtl number
R = residuals
Re = Reynolds number $\rho U_0 2H/\mu$
Ri = Richardson number; $g\beta\Delta Ts^3/\nu^2\mathrm{Re}^2$
s = step height
R = residuals
T = temperature
U_o = bulk velocity at the inlet
u = velocity component in x direction
v = velocity component in y direction
w = velocity component in z direction
W = channel width
$2H$ = channel height
$x_{\text{u-line}}$ = $x_{u\text{-line}}=[(du/dy)_{z=\text{const}}]|_{y=0}$
x, y, z = Coordinate directions

Subscripts

b = bulk, back
e = east
f = fluid
max = maximum
n = north
nb = neighborhood points
s = solid, south

t = top
0 = inlet
w = wall, west

Greek letters

α = underrelaxation factor
β = coefficient of thermal expansion
ε = convergence stop criteria
μ = dynamic viscosity
τ_{wx} = average streamwise shear stress
$\tau_{wx}=\mu(d\bar{u}/dy)_{y=o}$
υ = kinematic viscosity
ρ = density
ϕ = general variable (velocity and pressure)

References

[1] Iwai, H., Nakabe, K., Suzuki, K., and Matsubara, K., 2000, "Flow and heat transfer characteristics of backward-facing step laminar flow in a rectangular duct," Int. J. Heat Mass Transfer, **43**, pp. 457–471.

[2] Iwai, H., Nakabe, K., Suzuki, K., and Matsubara, K., 2000, "The effects of duct inclination angle on laminar mixed convective flows over a backward-facing step," Int. J. Heat Mass Transfer, **43**, pp. 473–485.

[3] Nie, J. H., and Armaly, B. F., 2002, "Three-Dimensional Convective Flow Adjacent to Backward-Facing Step Effects of Step Height," Int. J. Heat Mass Transfer, **45**, pp. 2431–2438.

[4] Blackwell, B. F., and Pepper, D. W., 1992, Benchmark problems for heat transfer codes, ASME-HTD-222, ASME, NY.

[5] Armaly, B. F., Li, A., and Nie, J. H., 2003, "Measurements in three-dimensional laminar separated flow," Int. J. Heat Mass Transfer, **46**, pp. 3573–3582.

[6] Nie, J. H., and Armaly, B. F., 2003, "Reattachment of three-dimensional flow adjacent to backward-facing step," ASME J. Heat Transfer, **125**, pp. 422–428.

[7] Carrington, D. B., and Pepper, D. W., 2002, "Convective heat transfer downstream of a 3D backward-facing step," Numer. Heat Transfer, Part A, **41**, pp. 555–578.

[8] Nie, J. H., and Armaly, B. F., 2002, "Buoyancy effects on three-dimensional convective flow adjacent to backward-facing step," J. Thermophys. Heat Transfer, **17**, pp. 122–126.

[9] Li, A., and Armaly, B. F., 2000, "Mixed convection adjacent to a 3D backward facing step," HTD-Proc. ASME Heat Transfer Division, **2**, pp. 51–58.

[10] White, F. M., 1991, *Viscous Fluid Flow*, 2nd ed., McGraw-Hill, New York

[11] Kakac, S., and Yener, Y., 1995, *Convective Heat Transfer*, 2nd ed., CRC Press, Boca Raton, FL.

[12] Shah, R. K., and London, A. L., 1978, *Laminar Flow Forced Convection in Ducts*, Academic Press, New York, USA

[13] Xi, C., and Han, P., 2000, "A Note on the Solution of Conjugate Heat Transfer Problems Using SIMPLE-like algorithms," Int. J. Heat Fluid Flow, **21**, pp 463–467.

[14] Patankar, S. V., 1980, *Numerical Heat Transfer and Fluid Flow*, Taylor and Francis, USA.

[15] Versteeg, H. K., and Malalasekera, W., 1995, *An Introduction to Computational Fluid Dynamics. The Finite Volume Technique*, Prentice-Hall, Malaysia.

[16] Guo, Z., and Anand, N. K., 1997, "Three-Dimensional Heat Transfer in a Channel with Baffle in the Entrance Region," Numer. Heat Transfer, Part A, **31**, pp. 21–35.

[17] Incropera, F. P., and Schutt, J. A., 1985, "Numerical Simulation of Laminar Mixed Convection in the Entrance region of Horizontal Rectangular Ducts," Numer. Heat Transfer, **8**, pp. 707–729.

[18] Luijkx, J. M., Platten, J. K., and Legros, J. C. L., 1981, "On the existence of thermoconvective rolls, transverse to a superimposed mean Poiseuille flow," Int. J. Heat Mass Transfer, **24**, pp. 1287–1291.